Journal of Power Sources 192 (2009) 279–284

Contents lists available at ScienceDirect

Journal of Power Sources

journal homepage: www.elsevier.com/locate/jpowsour

Novel Pd–Pb/C bimetallic catalysts for direct formic acid fuel cells

Xingwen Yu, Peter G. Pickup*

Department of Chemistry, Memorial University of Newfoundland, St. John's, Newfoundland, Canada A1B 3X7

ARTICLE INFO

Article history:
Received 9 February 2009
Received in revised form 17 March 2009
Accepted 18 March 2009
Available online 27 March 2009

Keywords:
Pd–Pb/C bimetallic catalyst
Direct formic acid fuel cell (DFAFC)
Synthesis
Stable catalytic activity
Characterization

ABSTRACT

Novel carbon supported bimetallic palladium–lead (Pd–Pb/C) anode catalysts have been prepared for use in direct formic acid fuel cells (DFAFC). Comparative studies, with a Pd/C catalyst, of performances, deactivation, and reactivation were performed in a multi-anode DFAFC. These Pd–Pb/C catalysts were found to be more resistant to deactivation in the DFAFC than Pd/C and to consistently show better long-term performances. With high purity formic acid, a Pd–Pb(4:1)/C catalyst also provided superior initial performance. Initial performances are more sensitive to acetic acid in the formic acid than for Pd/C. Both the Pd–Pb/C and Pd/C catalysts can be repeatedly reactivated by applying a −0.3 V cell potential for 5 s.
© 2009 Elsevier B.V. All rights reserved.

1. Introduction

Direct formic acid fuel cell (DFAFC) systems are currently under development as portable power sources for small electronic devices. Compared with other small fuel cell candidates, such as direct methanol fuel cells, DFAFCs have the advantages of high electromotive force, limited fuel crossover, and high practical power densities at low temperatures [1].

Both Pt-based and Pd-based catalysts have been used extensively in DFAFC anodes [1]. Pd black provides the best initial performance, but loses a large amount of its activity in a matter of hours [2,3]. Although Pd catalysts can easily be reactivated in the DFAFC [2–5], Pt-based catalysts such as Pt–Sn alloys [6] that show stable performances are better for continuous long-term operation. A key goal in DFAFC research is therefore to develop Pd-based anode catalysts that show both high and stable performances. This is particularly important in light of the much lower cost of Pd relative to Pt.

The rational development of stable Pd-based catalysts is made difficult by a lack of knowledge regarding how pure Pd deactivates during formic acid oxidation. Pt is known to deactivate rapidly due to the build-up of adsorbed CO [7–9], but no CO has been detected on Pd during formic acid oxidation [8,9]. The rate of deactivation of Pd depends strongly on the concentration of the formic acid [4] and on the presence of impurities such as acetic acid and methylformate [10]. It only occurs during formic acid oxidation, with the rate increasing sharply with decreasing cell voltage at low cell overpotentials, and then becoming stable for cell overpotentials greater than ca. 0.1 V [4].

The performances of Pt catalysts for formic acid oxidation have been improved by alloying or surface modification with metals known to promote CO oxidation via the so-called bifunctional mechanism. Pt–Ru and Pt–Sn are the best-known examples, and have been extensively studied for their CO tolerance in hydrogen fuel cells and their high activities in methanol fuel cells. Although Pt–Ru is generally considered to be superior to Pt–Sn in these applications [11,12], Pt–Sn is a much better catalyst for formic acid oxidation than Pt–Ru [6]. This indicates that the role of the second metal can be more complex than simple removal of CO at lower potentials. Bimetallic catalysts not known for their CO tolerance, such as Pt–Pd [7,13] and Pt–Au [14], have also shown enhanced activities over pure Pt for formic acid oxidation, as have Pt–Bi [15,16], Pt–As [17], Pt–In [15] and Pt–Pb [15,18,19].

In comparison to Pt-based catalysts, Pd-based bimetallic catalysts have received little attention for formic acid oxidation and use in DFAFCs. Larsen et al. reported that the addition of gold to Pd/C improves its activity [20]. Zhang et al. reported a Pd–P/C catalyst prepared via a solution phase synthesis with NaH_2PO_2 as a co-precursor [21]. Li and Hsing developed a novel synthesis method for a carbon supported Pd–Pt catalyst using a surfactant 3-(*N*,*N*-dimethyldodecylammonio)propanesulfonate (SB12) as the stabilizer [22].

This paper presents novel carbon supported bimetallic palladium–lead catalysts, Pd–Pb/C, for DFAFCs. These were discovered

* Corresponding author. Tel.: +1 709 737 8657.
E-mail address: ppickup@mun.ca (P.G. Pickup).

0378-7753/$ – see front matter © 2009 Elsevier B.V. All rights reserved.
doi:10.1016/j.jpowsour.2009.03.036

by screening of a number of chemically prepared catalysts in a DFAFC with nine independent anodes [4]. Pd–Pb catalysts were found to be superior to a commercial Pd/C catalyst as well as PdV, PdMo, and PdBi catalysts. Use of the multi-anode DFAFC allows the performances and deactivation of several different catalysts to be compared simultaneously. This is particularly important when deactivation occurs via an unknown agent and mechanism, since the effects of uncontrolled variations between experiments are avoided. Use of multiple electrodes of each type also allows for rapid assessment of the statistical significance of differences between catalysts.

2. Experimental

2.1. Preparation of catalysts

The 40% Pd–Pb/C bimetallic catalysts were synthesized by chemical reduction following solution phase impregnation of Pd(II) and Pb(II) into the carbon support. Aspects of several literature procedures [3,20,23] for the preparation of carbon supported Pd-based catalysts were combined and adapted in the development of the following procedure.

The Vulcan XC-72® carbon black support was pretreated by stirring in 10 M HNO_3 for 12 h and then rinsed with de-ionized water until the pH reached 6–7. A 200 mg sample of the treated support was then added to a solution made up of 42.2 mL of 8 g L^{-1} $Pd(NO_3)_2$ (Alfa Aesar, 39.86% Pd) solution with 10 drops of 10 M HNO_3, 2 mL of 5 g L^{-1} polyvinyl alcohol (PVA; Sigma–Aldrich), 25 mL of 10 g L^{-1} H_3BO_3, 5.4 mL (for an 8:1, Pd:Pb mass ratio) or 10.8 mL (for 4:1, Pd:Pb) of 5 g L^{-1} $Pb(NO_3)_2$, and 1 L of de-ionized water. The mixture was stirred vigorously while 50 mL of freshly prepared 5 g L^{-1} $NaBH_4$ in de-ionized water was added drop-wise. The pH was then adjusted to 9–10 by drop-wise addition of 5 M NaOH, and the mixture was stirred vigorously for a further 1 h. The product was then allowed to settle for 30 min, collected by filtration, rinsed well with de-ionized water and dried at 80 °C for 8 h under vacuum. A 40% Pd/C catalyst was synthesized by the same procedure without $Pb(NO_3)_2$. Combustion analysis (the residual mass following heating at 800 °C in air was taken due to Pd and PbO) gave metal loadings of 37.5% for the Pd/C catalyst, 45.3% for the Pd–Pb(4:1) catalyst, and 42.5% for the Pd–Pb(8:1) catalyst. Thus the Pd contents of all three catalysts were 37 ± 1%.

A commercial 40% Pd on C catalyst obtained from Etek was used in some experiments, as indicated.

2.2. Characterization of catalysts

2.2.1. Energy dispersive X-ray microanalysis (EDX)

EDX analyses of the catalysts were conducted on a Bruker Xflash 4010 SDD energy dispersive X-ray analyzer.

2.2.2. X-ray diffraction (XRD)

XRD patterns of the catalysts were obtained with an X-ray diffractometer (Rigaku D/Max-1400) using a Cu Kα source (λ = 0.15418 nm) at a scan rate of 1.5° min^{-1}. The scan range was from 30° to 100°.

2.2.3. Transmission electron microscopy (TEM)

TEM images of the catalysts were acquired with a JEOL 1200 EX transmission electron microscope at 60 keV. Samples for TEM measurements were prepared as follows: 2 mg of the catalyst was dispersed in 500 μl of ethanol by sonication for 30 min. A drop of the resulting ink was then deposited onto a carbon coated copper grid and dried at room temperature.

Table 1
Pd:Pb mass ratios from EDX and ICP-MS analysis.

	Targeted Pd:Pb	Pd:Pb from EDX	Pd:Pb from ICP-MS
Pd–Pb(4:1)/C	4:1	5.4 ± 0.3:1	3.7 ± 0.3:1
Pd–Pb(8:1)/C	8:1	10.1 ± 1.0:1	7.3 ± 1.3:1

2.3. Evaluation in a multi-anode fuel cell

2.3.1. Preparation of electrodes

The catalyst was dispersed in a mixture of pure water and a Nafion® solution (5%, DuPont) by sonication for 10 min. The mass ratio of net Nafion to the catalyst was 1:4 in all cases. The resulting ink was deposited onto carbon fiber paper (Toray TGP-H-090) and dried in air for 1 h at room temperature. The loading of the catalyst layer on the carbon fiber paper was 1.6 mg cm^{-2} (including carbon support and Nafion) in all cases. The metal loading (Pd + Pb) was nominally 0.51 mg cm^{-2} in all cases.

2.3.2. Multi-anode DFAFC and preparation of array anode membrane electrode assemblies (MEA)

A multi-anode, liquid-feed fuel cell that has been previously described [4] was used. It is based on a commercial (Electrochem®) 5 cm^2 active area cathode plate, and a custom anode plate with 9 (3 × 3 array) electronically isolated graphite rod anode current collectors embedded in a Lexan plate. Array anode membrane electrode assemblies were prepared by hot pressing (135 °C, 200 kg cm^{-2}, 90 s) a 5 cm^2 cathode consisting of 4 mg cm^{-2} Pt black on carbon fiber paper, and nine 0.23 cm^2 anodes onto a Nafion 115® membrane (Ion Power).

2.3.3. Cell performance tests

The operation of the multi-anode DFAFC was controlled with a multi-channel potentiostat (Arbin®). The cell was operated with 5 M aqueous formic acid fed to the anode at a flow rate of 0.2 ml min^{-1}, and dry oxygen delivered to the cathode at a flow rate of 100 sccm without back pressure. The cell was conditioned at open circuit for typically 1 h before experiments. Then a polarization experiment to 0.3 V was performed to check performance, and the anodes were reactivated by applying a cell voltage of −0.3 V for 5 s. Reactivation was performed in this way between all subsequent experiments, except between polarizations in consecutive polarization experiments. Polarization experiments were run from the initial open circuit voltage (OCV) to 0.3 V in 15 mV steps with 30 s for the current to stabilize at each cell voltage. Consecutive polarizations were collected without any pause or treatment between them. All experiments were conducted at ambient temperature.

3. Results and discussion

3.1. Characterization of the catalysts

The mass ratios of Pd to Pb in the catalysts (Table 1) obtained by EDX were somewhat higher than the targeted values, while ICP-MS gave slightly lower values. Considering the inherent uncertainty in EXD data, the analyses do not indicate that there were significant deviations from the targeted compositions.

Fig. 1 presents XRD patterns of the Pd–Pb(4:1)/C and the Pd–Pb(8:1)/C catalysts, as well as the Pd/C catalyst for comparison. While the main Pd peaks at 40.1°, 46.7°, 68.1° and 82.1° are obvious for each catalyst, no Pb peaks can be seen. This indicates that the Pb was either in an amorphous state, or alloyed with the Pd. The addition of Pb caused clear shifts of the Pd peaks for both catalysts (Table 2), with the effect being greater for the higher Pb content, which indicates that alloying had occurred.

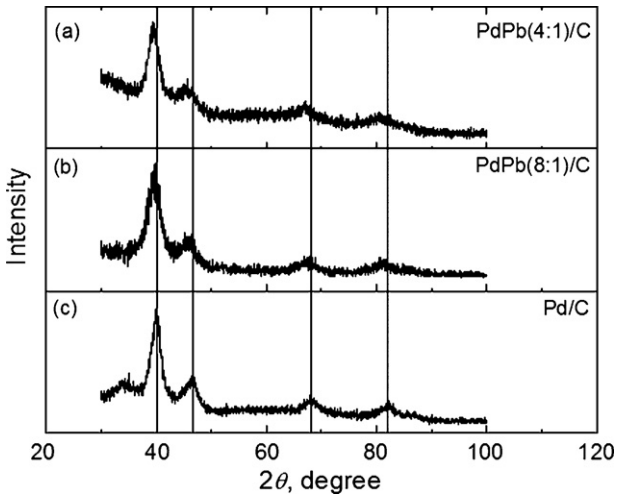

Fig. 1. XRD patterns of the catalysts: (a) Pd–Pb(4:1)/C; (b) Pd–Pb(8:1)/C; (c) Pd/C.

Table 2
Pd XRD peak positions and shifts, and mean crystallite sizes for the Pd/C and Pd–Pb/C catalysts.

Pd/C	Pd–Pb(4:1)/C		Pd–Pb(8:1)/C	
Position (°)	Position (°)	Shift (°)	Position (°)	Shift (°)
40.1	39.6	−0.5	39.8	−0.3
46.7	46.0	−0.7	46.3	−0.4
68.1	67.3	−0.8	67.8	−0.3
82.1	80.9	−1.2	81.0	−1.1
Particle size (nm)				
4.2	3.5		3.4	

Crystallite sizes, estimated by using the Scherrer equation, are listed in Table 2. There was no evident crystallite size difference between the two Pd–Pb/C bimetallic catalysts, but the average crystallite size for the Pd/C catalyst without Pb was a little larger. The particle size and distribution for the Pd–Pb(4:1)/C catalyst was also investigated by TEM. As shown in Fig. 2, the Pd–Pb particles were evenly distributed on the carbon support. The average particle sizes seen in TEM images were reasonably consistent with the crystallite size estimated by XRD, although a quantitative comparison was not made.

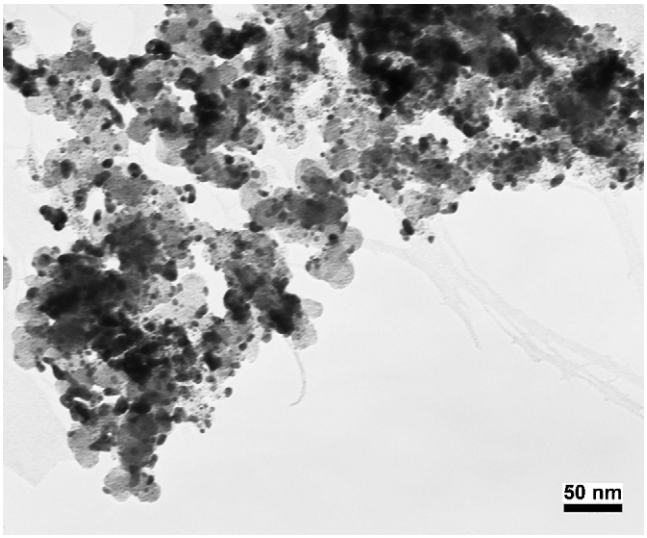

Fig. 2. TEM image of the Pd–Pb(4:1)/C catalyst.

3.2. Performance of Pd–Pb/C bimetallic catalysts

Recently, the poisoning of palladium catalysts in direct formic acid fuel cells by impurities in the formic acid fuel has been reported [10,24]. Since different impurities may affect each catalyst separately and all grades/sources of formic acid contain impurities, it is prudent to compare catalysts with several different grades/sources. In addition, the use of a lower grade of formic acid can accelerate deactivation and speed-up the screening of catalysts. In this study, we therefore employed two types of formic acid as the fuel, Alfa Aesar® ACS formic acid (Lot# H13S025) and Fluka HPLC grade formic acid (Lot# 09076). The Alfa Aesar product contained a relatively large concentration of acetic acid (estimated to be ca. 3300 ppm (mass basis) by proton NMR following the procedure in Ref. [24]; no methylformate was detected), which has been shown to decrease the initial current in a DFAFC [10,24] and accelerate the rate of deactivation of Pd anodes [10]. In contrast, the Fluka HPLC formic acid was found to contain <1 ppm acetic acid and ca. 15 ppm methylformate. This level of impurities should not significantly affect the performance of the DFAFC [10,24].

3.2.1. Cell performance with Alfa Aesar® formic acid

Fig. 3 shows data from sets of consecutive polarization curves run on a multi-anode DFAFC with five Pd/C and four Pd–Pb(4:1)/C anodes. Twelve polarization experiments were run continuously with the cell voltage being returned to the initial OCV at the end of each run and no pause or reactivation between runs. For clarity, only the 1st, 6th, and 12th sets of polarization data are shown, and since many of the individual polarization curves overlap, data for each type of catalyst are shown as two lines representing the average ± s (standard deviation). As well as providing better clarity, this allows for facile judgment of the reproducibility of the results as well as the statistical significance of differences between catalysts. The collection of such statistical data is one of the key advantages of the multi-anode cell.

The reproducibility of the polarization curves between electrodes of the same type was excellent for the Pd–Pb(4:1)/C catalyst but more variable for the Pd/C catalyst. There was a notable divergence of the performances of the individual Pd/C electrodes as the experiment progressed. This is seen most clearly in Fig. 3 for the 12th polarization, where the two dashed lines encompass a wide

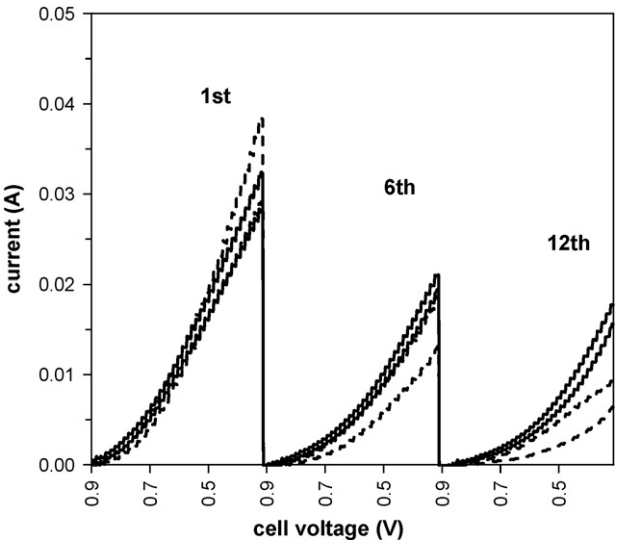

Fig. 3. Ranges (average ± s) for the 1st, 6th, and 12th of 12 consecutive polarization curves for five Pd/C electrodes (dashed lines) and four Pd–Pb(4:1)/C electrodes (solid lines) in a multi-anode DFAFC with 5 M Alfa Aesar formic acid. The total test time was 4 h.

range of performances. This type of difference in reproducibility between the PdPd/C and Pd/C catalysts was seen throughout this work, and can be attributed to variations in the deactivation rates of the individual electrodes. Possible reasons could include slight differences in the concentrations of impurities experienced by each electrode and slight variations in catalyst loadings.

Initially (during the first polarization experiment shown in Fig. 3), the Pd–Pb(4:1)/C and Pd/C catalysts gave similar performances, with no statistically significant differences. Both catalysts deactivated slowly during repeated polarization experiments, but the decrease was much more pronounced for the Pd/C anodes. In Fig. 3, the difference became statistically significant (defined here as no overlap between the standard deviation ranges shown in the figure) for the 6th polarization. At the end of the 12th polarization, the average current at the Pd/C electrodes was less than half of that at the Pd–Pb/C electrodes. It is clear that the addition of Pb to Pd stabilizes it significantly to deactivation during formic acid oxidation. It is also important to note that the performances and deactivation rates reported here for the Pd/C catalyst prepared in this work are comparable to previous results obtained with a 40% Pd/C commercial catalyst [4].

Fig. 4 compares the deactivation rates of the Pd–Pb(4:1)/C and Pd/C catalysts during operation of the cell at a fixed voltage of 0.3 V. Here data for all nine electrodes are shown to illustrate reproducibility. Although the initial currents ($t < 100$ s) for the Pd–Pb(4:1)/C catalyst were lower than for the Pd/C catalyst, the current decay was much slower. Consequently, the performances of the Pd–Pb(4:1)/C anodes exceeded those of the Pd/C anodes after ca. 2 h of continuous cell operation. After 4 h of operation, the current densities for the Pd–Pb(4:1)/C anodes were on average 2.4 times those for the Pd/C anodes.

It is pertinent to note that in Fig. 4, four of the Pd electrodes and three of the Pd–Pb electrodes displayed excellent reproducibility, while one electrode of each type gave anomalously high (Pd–Pb) or low (Pd) currents during the first 10,000 s. The observation of anomalies highlights the importance of using multiple electrodes of each type. Interestingly, the currents at the anomalous electrodes became consistent with those at the other electrodes by the end of the experiment. The source of anomalies such as these is a mystery,

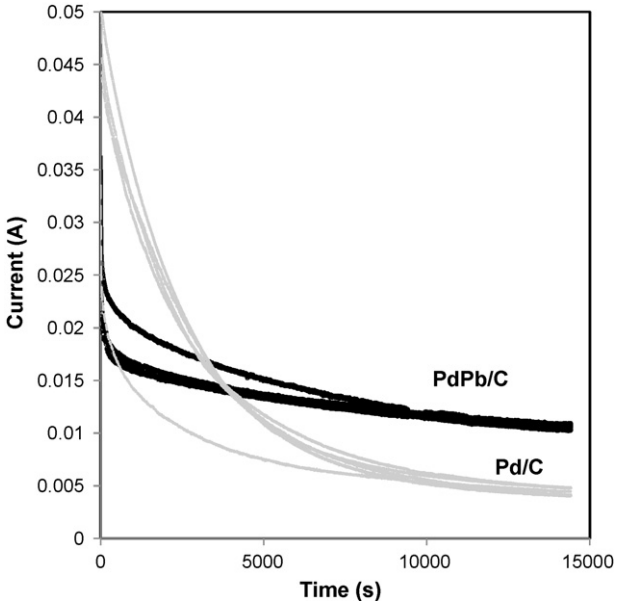

Fig. 4. Current vs. time plots for five Pd/C electrodes (light lines) and four Pd–Pb(4:1)/C electrodes (heavy lines) at 0.3 V vs. the cathode in a multi-anode DFAFC with 5 M Alfa Aesar formic acid.

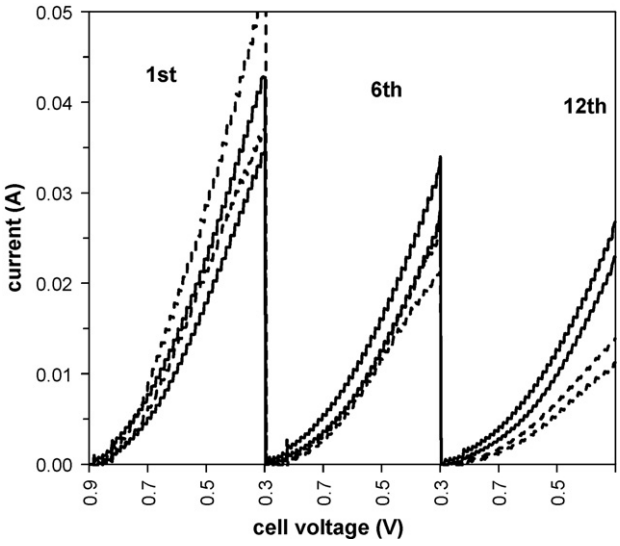

Fig. 5. Ranges (average ± s) for the 1st, 6th, and 12th of 12 consecutive polarization curves for four Pd/C electrodes (dashed lines) and five Pd–Pb(4:1)/C electrodes (solid lines) in a multi-anode DFAFC with 5 M Fluka HPLC formic acid. The total test time was 4 h.

and cannot be attributed to "bad" electrodes (since they behaved normally in other experiments) nor to position in the array (since different electrodes behaved anomalously in other experiments and arrays).

3.2.2. Cell performance with Fluka HPLC grade formic acid

As a high purity formic acid product, the HPLC grade formic acid has been reported to have good compatibility with palladium-based catalysts in a DFAFC [10,24]. As shown in Fig. 5, both the Pd–Pb(4:1)/C and Pd/C catalysts provided better cell performance than with the Alfa Aesar formic acid (Fig. 3). It is also seen that the Pd–Pb(4:1)/C catalyst exhibited much slower performance decays than the Pd/C catalyst during repeated polarization experiments.

For the Pd/C electrodes in Figs. 3 and 5, the average current at 0.3 V in the first polarization experiment was 25% lower for the Alfa Aesar than for the HPLC formic acid. This is similar to the effect expected for the ca. 3300 ppm of acetic acid in the Alfa Aesar product [10,24], suggesting that other impurities do not influence the performance of the fuel cell greatly. The rate of deactivation of the Pd/C electrodes was similar for the two types of formic acid, however, with a 72% decrease in the average current at 0.3 V for the 12th polarization with HPCL formic acid and a 77% decrease with Alfa Aesar formic acid. This is consistent with a recent report that acetic acid lowers the initial performance of a DFAFC, but does not significantly affect the deactivation rate [24]. However, it has also been reported that acetic acid can increase the rate of deactivation [10]. This discrepancy may be due to differences in the experimental protocols, since differing effects of acetic acid on deactivation are seen here (see below) depending of the experimental method (polarization vs. constant current).

Fig. 6 compares the DFAFC currents with the Pd–Pb(4:1)/C and Pd/C catalysts at a constant cell voltage of 0.3 V. Again, the current decay is much slower for the Pd–Pb(4:1)/C catalyst than for the Pd/C catalyst. After 4 h of operation, the current density at the Pd–Pb(4:1)/C anodes was on average 1.8 times higher than at the Pd/C anodes.

By comparing Figs. 4 and 6, it can be seen that the quality of the formic acid plays a large role in the performance of the DFAFC and in the rate of catalyst deactivation. At a constant cell voltage of 0.3 V, initial currents (taken at 10 s to avoid contributions from the charging current) at the Pd electrodes were 25% lower with Alfa

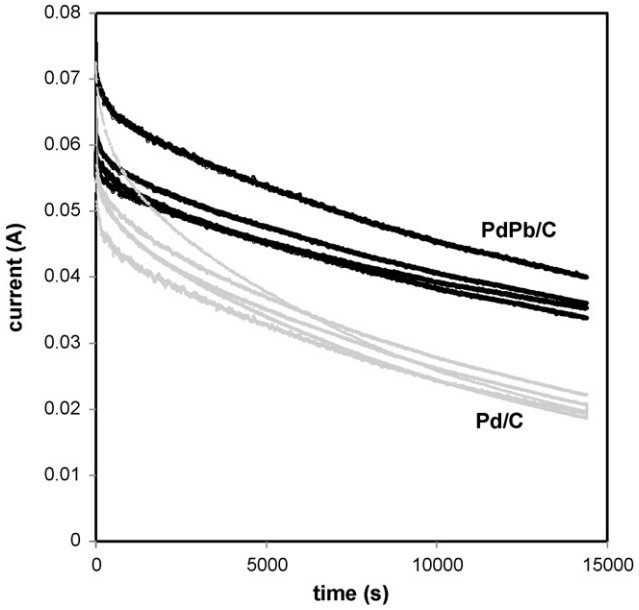

Fig. 6. Current vs. time plots for four Pd/C electrodes (light lines) and five Pd–Pb(4:1)/C electrodes (heavy lines) at 0.3 V vs. the cathode in a multi-anode DFAFC with 5 M Fluka HPLC formic acid.

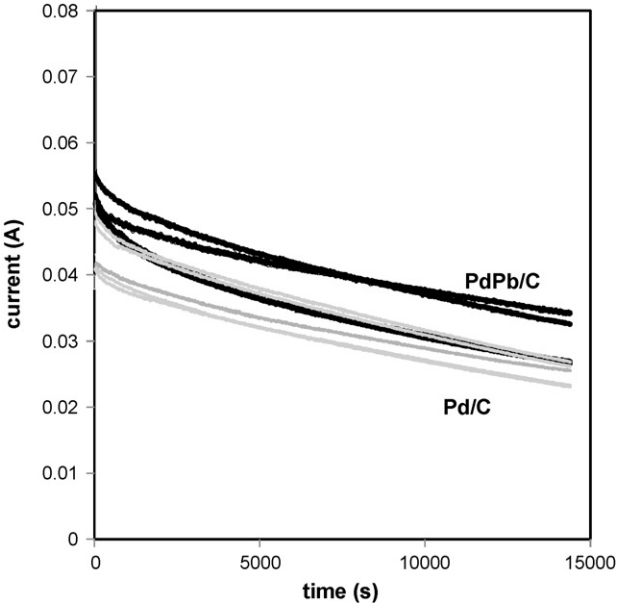

Fig. 7. Current vs. time plots for five Pd/C electrodes (light lines) and four Pd–Pb(8:1)/C electrodes (heavy lines) at 0.3 V vs. the cathode in a multi-anode DFAFC with 5 M Fluka HPLC formic acid.

Aesar formic acid (compare Figs. 4 and 6), which is consistent with the difference seen at 0.3 V in the first polarization experiments (Figs. 3 and 5). For the Alfa Aesar formic acid, the decay over 4 h was significantly higher at a constant voltage than during polarizations, with currents decreasing by 90% for the Pd electrodes in Fig. 4. In contrast, the decay at constant voltage was only 66% for the Pd electrodes with HPLC formic acid (Fig. 6).

For the Pd–Pb(4:1)/C anodes, the quality of the formic acid influenced the initial performance greatly, with a 58% lower average current at 10 s for Alfa Aesar formic acid relative to HPLC formic acid. However, the rate of decay was less sensitive to the impurities (mainly acetic acid) in the Alfa Aesar product, with only a 60% decay over 4 h relative to 42% with HPLC formic acid.

These results clearly show differences in the effects of impurities on the Pd and Pd–Pb catalysts. At this stage the origins of these differences are unclear, but it can be concluded that the presence of Pb enhances long-term resistance to the effects of acetic acid (Fig. 4), and that Pd–Pb can provide better initial performances than Pd when high purity formic acid is used, as well as providing some resistance to deactivation (Fig. 6). Further investigation may help in the understanding of why Pd electrodes deactivate during formic acid oxidation.

A PdPd catalyst with a lower Pb content, Pd–Pb(8:1)/C, was also evaluated. Both repeated polarization experiments (not shown) and constant cell voltage experiments (e.g. Fig. 7) demonstrated that Pd–Pb(8:1)/C was more resistance to deactivation than Pd/C. With Alfa Aesar formic acid, the Pd–Pb(8:1)/C catalyst provide significantly better short term performances than the Pd–Pb(4:1)/C catalyst while performances were similar after 4 h. In contrast, the Pd–Pb(4:1)/C outperformed the Pd–Pb(8:1)/C catalyst at all times when HPLC formic acid was used (compare Figs. 6 and 7). Overall, the best DFAFC performance obtained was that shown in Fig. 6 for Pd–Pb(4:1)/C and HPLC formic acid.

3.3. Reactivation of electrodes

Since the Pd–Pb/C catalysts reported here do still deactivate in the DFAFC they will need to be regularly reactivated if used in a commercial fuel cell system, as required currently for Pd catalysts. Reactivation can be achieved under the same conditions used for Pd/C. The most convenient way to do this is to set the cell potential to −0.3 V for 5 s [4], although other protocols involving use of a dynamic hydrogen cathode have generally been used [2,3,5].

One concern about the use of alloy catalysts is that the highly oxidizing conditions required for reactivation could cause partial dissolution of the catalyst particles and changes in their surface composition. The resistance of both a Pd–Pb/C catalyst and Pd/C catalyst to repeated deactivation and reactivation was therefore investigated. A commercial 40% Pd/C catalyst was used here in order to show a comparison with the Pd–Pb(4:1)/C catalyst.

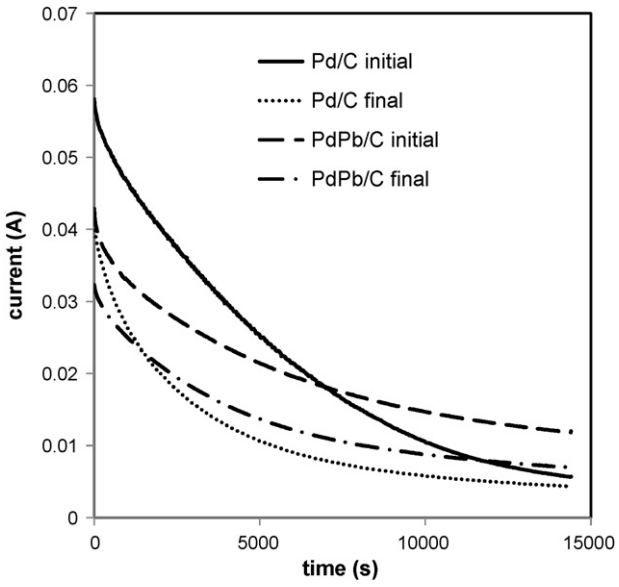

Fig. 8. Average current vs. time plots before and following 14 deactivation/reactivation (at −0.3 V for 5 s) cycles for four Pd/C (Etek) electrodes and five Pd–Pb(4:1)/C electrodes at 0.3 V vs. the cathode in a multi-anode DFAFC 5 M with Alfa Aesar formic acid. The initial curves were obtained following reactivation after a consecutive polarization experiment, while the final curves were recorded following a further 14 deactivation (4 h at 0.3 V)/reactivation (5 s at −0.3 V) cycles.

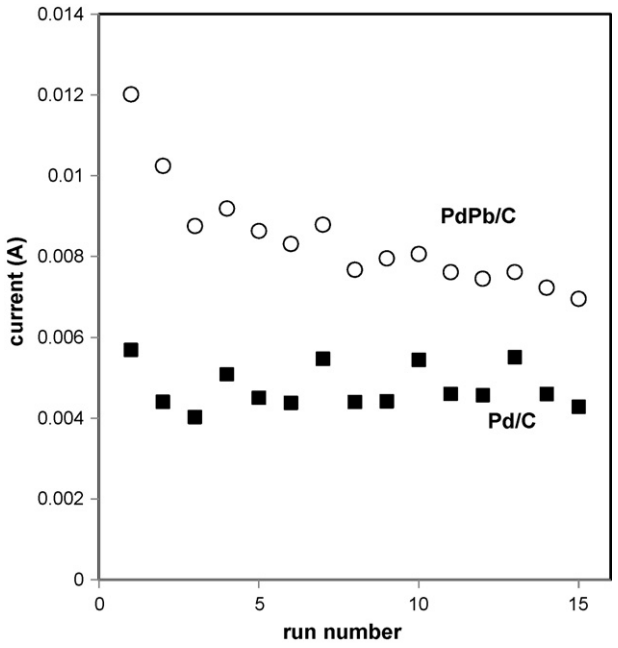

Fig. 9. Average currents after 4 h at 0.3 V vs. run number for four Pd/C (Etek) electrodes and five Pd–Pb(4:1)/C electrodes in a multi-anode DFAFC with 5 M Alfa Aesar formic acid. The electrodes were reactivated at −0.3 V for 5 s between each run.

Fig. 8 shows current vs. time curves obtained before and following 14 deactivation/reactivation cycles. It can be seen that the performances of both the Pd/C and Pd–Pb(4:1)/C catalysts deteriorated following repeated reactivation. At short times, the effect was greater for Pd/C, while at longer times it was greater for Pd–Pb(4:1)/C. Nevertheless, the Pd–Pb(4:1)/C maintained its long-term superiority over Pd/C, and actually become superior over a longer fraction of the operating time.

Fig. 9 shows the average current after 4 h of operation for each type of electrode as a function of cycle number. It can be seen that the Pd/C catalyst exhibited better stability in its long-term performance, although it remained inferior to the Pd–Pb(4:1)/C. Long-term degradation of the Pd–Pb(4:1)/C is clearly an issue, however. Better stability may be possible with less aggressive reactivation conditions [5], or use of better quality formic acid.

4. Conclusions

Pd–Pb/C catalysts can provide superior initial performance in a DFAFC relative to Pd/C and are more resistant to deactivation. They are therefore better candidates for use in commercial systems. Both types of catalyst can easily be reactivated, but suffer long-term activity loss that may not be recoverable. Impurities, particularly acetic acid, play a role in the deactivation of both types of catalyst although there are differences in how each catalyst is affected. The initial performance of the Pd–Pb/C catalysts is most susceptible to impurities, while the deactivation rate is influenced more for Pd/C.

Acknowledgements

This work was supported by the Natural Sciences and Engineering Research Council of Canada (NSERC) through a Strategic Projects Grant in partnership with Tekion (Canada) Inc., and by Memorial University.

References

[1] X. Yu, P.G. Pickup, J. Power Sources 177 (2008) 124.
[2] S. Ha, R. Larsen, Y. Zhu, R.I. Masel, Fuel Cells 4 (2004) 337.
[3] Y.M. Zhu, Z. Khan, R.I. Masel, J. Power Sources 139 (2005) 15.
[4] X. Yu, P.G. Pickup, J. Power Sources 187 (2008) 493.
[5] Y. Pan, R. Zhang, S.L. Blair, Electrochem. Solid State Lett. 12 (2009) B23.
[6] C. Iordache, S. Blair, D. Lycke, S.P. Huff, World Patent (2008) WO 2008/080227 Al.
[7] C. Rice, S. Ha, R.I. Masel, A. Wieckowski, J. Power Sources 115 (2003) 229.
[8] M. Arenz, V. Stamenkovic, T.J. Schmidt, K. Wandelt, P.N. Ross, N.M. Markovic, Phys. Chem. Chem. Phys. 5 (2003) 4242.
[9] M. Arenz, V. Stamenkovic, P.N. Ross, N.M. Markovic, Surf. Sci. 573 (2004) 57.
[10] R.I. Masel, Y. Zhu, Z. Khan, M. Man, UK Patent (2007) GB2424650B.
[11] S. Wasmus, A. Kuver, J. Electroanal. Chem. 461 (1999) 14.
[12] H.S. Liu, C.J. Song, L. Zhang, J.J. Zhang, H.J. Wang, D.P. Wilkinson, J. Power Sources 155 (2006) 95.
[13] P. Waszczuk, T.M. Barnard, C. Rice, R.I. Masel, A. Wieckowski, Electrochem. Commun. 4 (2002) 599.
[14] J.H. Choi, K.J. Jeong, Y. Dong, J. Han, T.H. Lim, J.S. Lee, Y.E. Sung, J. Power Sources 163 (2006) 71.
[15] E. Casado-Rivera, D.J. Volpe, L. Alden, C. Lind, C. Downie, T. Vazquez-Alvarez, A.C.D. Angelo, F.J. DiSalvo, H.D. Abruna, J. Am. Chem. Soc. 126 (2004) 4043.
[16] A.V. Tripkovic, K.D. Popovic, R.M. Stevanovic, R. Socha, A. Kowal, Electrochem. Commun. 8 (2006) 1492.
[17] E. Herrero, A. Fernandez-Vega, J.M. Feliu, A. Aldez, J. Electroanal. Chem. 350 (1993) 73.
[18] L.R. Alden, D.K. Han, F. Matsumoto, H.D. Abruna, F.J. DiSalvo, Chem. Mater. 18 (2006) 5591.
[19] D.M. dos Anjos, F. Hahn, J.M. Leger, K.B. Kokoh, G. Tremiliosi, J. Solid State Electrochem. 11 (2007) 1567.
[20] R. Larsen, S. Ha, J. Zakzeski, R.I. Masel, J. Power Sources 157 (2006) 78.
[21] L.L. Zhang, Y.W. Tang, J.C. Bao, T.H. Lu, C. Li, J. Power Sources 162 (2006) 177.
[22] X.G. Li, I.M. Hsing, Electrochim. Acta 51 (2006) 3477.
[23] L.L. Zhang, T.H. Lu, J.C. Bao, Y.W. Tang, C. Li, Electrochem. Commun. 8 (2006) 1625.
[24] W.L. Law, A.M. Hack, P.D.C. Wimalaratne, S.L. Blair, Electrochem. J. Soc. 156 (2009) B553.